Novel whole blood assay for phenotyping platelet reactivity in mice identifies ICAM-1 as a mediator of platelet-monocyte interaction

Paul C.J Armstrong PhD[1], Nicholas S. Kirkby PhD[1,2], Melissa V. Chan PhD[1], Michaela Finsterbusch PhD[1], Nancy Hogg PhD[3], Sussan Nourshargh PhD[1], Timothy D. Warner PhD[1]

[1]William Harvey Research Institute, Barts & the London School of Medicine & Dentistry, Queen Mary University of London, Charterhouse Square, London, EC1M 6BQ, UK

[2]National Heart & Lung Institute, Imperial College London, Dovehouse Street, London, SW3 6LY, UK

[3]Leukocyte Adhesion Laboratory, Cancer Research United Kingdom, London Research Institute, London WC2A 3LY, UK

Corresponding Author:

Dr Paul Armstrong

William Harvey Research Institute

Barts & the London School of Medicine & Dentistry

Charterhouse Square

LONDON

EC1M 6BQ

UK

Email, p.c.armstrong@qmul.ac.uk

Running Title: Mouse platelet phenotyping

Key Points:

Low volume, high throughput whole blood aggregometry will facilitate future mouse platelet function research.

Application of this approach identifies ICAM-1 as a novel mediator of platelet-monocyte interaction through fibrinogen binding.

Abstract

Testing of platelet function is central to the cardiovascular phenotyping of genetically modified mice. Traditional platelet function tests have been developed primarily for testing human samples and the volumes required make them highly unsuitable for the testing of mouse platelets. This limits research in this area. To address this problem we have developed a miniaturised whole blood aggregometry assay, based on a readily accessible 96-well plate format coupled with quantification of single platelet depletion by flow cytometric analysis. Using this approach we observed a concentration-dependent loss of single platelets in blood exposed to arachidonic acid, collagen, U46619 or protease activated receptor (PAR) 4 activating peptide. This loss was sensitive to well established antiplatelet agents and genetic manipulation of platelet activation pathways. Observations were more deeply analysed by flow cytometric imaging, confocal imaging, and measurement of platelet releasates. Phenotypic analysis of the reactivity of platelets taken from mice lacking intercellular adhesion molecule (ICAM) 1 identified a marked decrease in fibrinogen-dependent platelet monocyte interactions, especially under inflammatory conditions. Such findings exemplify the value of screening platelet phenotypes of genetically modified mice and shed further light upon the roles and interactions of platelets in inflammation.

Introduction

Platelets are key mediators of haemostasis. They have crucial roles in certain bleeding disorders and are the targets of anti-thrombotic therapies, notably aspirin and $P2Y_{12}$ receptor blockers, such as clopidogrel[1-3]. Numerous assays have been developed to investigate platelet responses with an understandable focus on analysing human clinical samples[4,5]. These assays require relatively large volumes of blood with the majority requiring a sample volume in excess of 200µl per test[6].

Mouse models are widely used in cardiovascular research, particularly for phenotyping of genetic modifications and testing novel therapeutic agents. However, platelet function testing in mice remains difficult since a complete and terminal blood collection provides at

most 1ml of blood. Further, commonly used strategies for extending the volume available such as dilution or platelet washing can introduce artefactual changes in platelet responses and thus does not permit study of platelet interactions with other blood cells and constituents. As a result both the number and type of platelet tests that can be performed in samples from mice are severely limited, diminishing the experimental value of each mouse and making detailed study of mouse platelets impractical. There is therefore a clear and pressing experimental demand for murine-focused and optimised functional assays.

We have previously developed the 'Optimul' assay for measuring platelet aggregation in low volumes (40µl) of platelet-rich plasma[7,8], and have very recently reported its utility in the testing of platelet function patients with bleeding disorders[9]. However, the 'Optimul' system relies on optical measurement of sample turbidity to assess platelet aggregation, making it unsuitable for analysis of platelet function in whole blood. Several studies have demonstrated platelet counting to be a viable alternative method for monitoring platelet aggregation, since single platelets are 'consumed' into larger aggregates upon activation[10-12]. Similarly it has also previously been demonstrated that flow cytometry can be used to determine platelet counts in ~5µl of blood by reference to known amounts of enumeration beads[13]. With flow cytometry now widely available, such an approach provides an attractive and viable solution for determining platelet aggregation in low-volumes of blood.

By combining *ex vivo* stimulation of platelets in small volumes of whole blood in 96-well plates with flow cytometric counting of single platelets, we have developed a novel and accessible experimental approach for *ex vivo* platelet function testing in mice. Here, we confirm the sensitivity and specificity of this assay by demonstrating its ability to detect pharmacological and genetic interruption of well-established and clinically relevant platelet activation pathways involving the $P2Y_{12}$ receptor and cyclo-oxygenase (COX)-1.

Moreover, given that platelet reactivity is studied in a whole blood setting, we applied this novel assay to examine the platelet response phenotype in whole blood of mice lacking adhesion receptors. Crucially we identified intracellular adhesion molecule (ICAM) 1, through fibrinogen binding, as a previously unreported mediator of platelet-monocyte interactions.

Materials and Methods

Mouse strains

COX-1 knockout (KO), and ICAM-1 mice were previously generated on a C57Bl/6J background and identified by genomic PCR as described[14,15]. C57Bl/6 wild type (WT) mice

were purchased from Charles River UK. All mice were aged between 8-12 weeks (20-25g) and housed for a minimum of 7 days before commencement of experiments. They were housed on a 12-hour light-dark cycle, at a temperature of 22-24°C with access to water and food *ad libitum*. Animal procedures were conducted in accordance with Home Office legislation under "The Animals (Scientific Procedures) Act 1986" and were subject to local approval from Queen Mary University of London and Imperial College London Ethical Review Panels.

Collection of blood and preparation of platelet rich plasma

Blood was collected from the inferior vena cava into either lepirudin (Refludan™, 25 µg/ml; Celgene, Windsor, UK), sodium citrate (0.32%; Sigma, Poole, UK) or heparin (10U/ml; Wockhardt, Wrexham, UK) from mice anesthetized with ketamine (Narketan®, 100 mg/kg; Vetoquinol, UK) and xylazine (Rompun®, 10 mg/kg; Bayer, Kiel, Germany). Platelet rich plasma (PRP) was isolated as previously published by Woulfe *et al*[16]. Briefly, whole blood was diluted 1:1 with HEPES-tyrodes buffer (37 mM NaCl, 20 mM HEPES, 5.6 mM glucose, 1 g/l BSA, 1 mM $MgCl_2$, 2.7 mM KCl, 3.3 mM NaH_2PO_4) before centrifugation (100 *g*, 8mins, RT).

Platelet or whole blood stimulation

Half-area 96-well microtitre plates (Greiner Bio-One, Stonehouse, UK) were pre-coated with hydrogenated gelatine (0.75% w/v; Sigma, UK) in PBS to block non-specific activation of blood. 4µl of vehicle or agonist solution was then added to each well: arachidonic acid (AA; 0.05–0.5mM; Sigma, Poole, UK), Horm collagen (0.1–10µg/ml; Nycomed, Linz, Austria), the PAR-4 activating peptide AYPGKF amide (PAR4-amide, 50–100mM; Bachem, Bubendorf, Switzerland), and the stable thromboxane (Tx) A_2 mimetic U46619 (0.1–10µM; Cayman Chemical Company, Ann Arbor, USA). These platelet agonists are most widely used in *in vitro* platelet testing[17].

To each well, 35µl of PRP or whole blood was added and the plate was then placed onto a heated plate shaker (Bioshake IQ, Q Instruments, Jena, Germany) at 37°C for 5 mins mixing at 1200rpm. Where appropriate, light transmission of each well was determined using a 96-well plate reader (Sunrise™, Tecan, Mannedorf, Switzerland) at 595nm. Following mixing, 5µl was removed from each well and diluted 1:10 into an acid citrate dextrose solution (5mM glucose, 6.8 mM trisodium citrate, 3.8 mM citric acid). In some experiments, blood was pre-treated with the $P2Y_{12}$ receptor blocker prasugrel-active metabolite (PAM; 30µM) or its vehicle (0.5% DMSO) for 30 mins at 37 °C. Alternatively, blood was pre-incubated with prostacyclin (PGI_2, Epoprostenol, 2µg/ml; Tocris bioscience, Abingdon, UK) for 1 min

immediately before agonist stimulation. In ICAM-1 KO experiments whole blood was pre-incubated with murine TNF-α (20ng/ml; Life Technologies, Paisley, UK), eptifibatide (10μg/ml) or Fibrinogen γ-Chain 117-133 (20μM; Bachem, Switzerland, for both).

Flow cytometry

Individual platelet counts of each well were determined according to Alugupalli *et al*[13]. Briefly, platelets were labelled with FITC or APC conjugated anti-CD41 (clone eBioMWReg30) or anti-CD42d-PE (clone 1C2) monoclonal antibodies (eBioscience, Hatfield, UK) for 30 mins. Samples were then diluted 1:50 in phosphate buffered saline containing 0.1% formalin (Sigma, UK), 0.1% dextrose and 0.2% bovine serum albumin (BSA) before addition of 10^4 CountBright™ absolute counting beads (Life Technologies). Labelled, diluted blood was then analysed using a FACSCalibur flow cytometer (BD Biosciences, Oxford, UK).

For more in-depth analysis of cell-interactions an ImageStream^X MarkII imaging flow cytometer was used, as this combines the quantitative power of flow cytometry with high content image analysis by acquiring up to twelve images simultaneously of each cell or object including brightfield, scatter, and multiple fluorescent images. Images were analysed using IDEAS software (Amnis, Seattle, WA). To prepare samples, whole blood samples were stained with anti-CD41-FITC (platelets), anti-CD45-PE (leukocytes, clone 30F11), and anti-Ter119-APC (erythrocytes clone Ter-119, all Miltenyi Biotec, Bisley, UK) then fixed and diluted in a formalin/PBS solution containing dextrose and BSA. To study platelet-monocyte interactions, whole blood samples were fixed and erythrocytes removed using Lyse/Fix (BD Bioscience) before staining with anti-CD42d-PE, anti-mouseLy6C-APC (clone HK1.4, eBioscience) for monocytes or anti-mouseCD54 (clone YN1/1.7.4) for ICAM-1.

Confocal microscopy

Blood was stimulated as described above. Platelets were stained using a rat anti-mouse CD42c-DyLight488 antibody (Emfret, Eibstadt, Germany). Cells were fixed and red blood cells were lysed using commercially available 1-step Fix/Lyse (eBioscience). Neutrophils were then stained for intracellular MRP-14 (S100A9), using a goat anti-MRP-14 polyclonal antibody conjugated to Alexa Fluor 555 (R&D systems, Abingdon, UK). Immunofluorescent-labelled cells were imaged using a Zeiss LSM 5 PASCAL confocal laser-scanning microscope incorporating an x63 oil-dipping objective (numerical aperture 1.4). Z-stack images were acquired using the multiple track scanning mode at a resolution of 1,024 × 1,024 pixels in the $x \times y$ plane and 0.4μm steps in z direction. Resulting 3D confocal images were then analysed using the image processing software IMARIS (Bitplane, Zurich, Switzerland).

Analysis of thromboxane A_2 production

Following stimulation of whole blood samples, COX activity was halted by the addition of 1 mM diclofenac (Sigma), the samples were centrifuged at 1300 *g* for 10 min at 5°C. Plasma supernatants were then removed and stored at -80^{o}C. Thromboxane (TX) B_2 levels in the supernatant, as a measure of TXA_2 formation, were determined by selective ELISA (Cayman Chemical, Ann Arbour, USA).

Statistics and data analysis

Data presented as mean ±SEM, and analysed using FlowJo v7.4 (Treestar, Ashland, USA) and Prism 5.01 (GraphPad software, USA). For analysis, the "single platelet" population was gated based on forward scatter and anti-platelet immunoreactivity (fluorescence intensity). Statistical significance was determined by two-way ANOVA with Dunnett's post-hoc test unless otherwise stated, and data sets considered different if $p<0.05$. Each n value represents a data point from a separate animal.

Results and discussion

Detection of single platelets and agonist-induced platelet aggregation

In order to establish a viable platelet aggregation assay based on the platelet counting technique it was first necessary to demonstrate the robust detection of single platelets in whole blood and determine their fate upon stimulation with platelet activating substances. By flow cytometry analysis, a population of sub-cellular sized particles immunoreactive to the platelet marker CD41 (GPIIb) was clearly detected in unstimulated blood[13] (Figure 2a). Mixing of blood in a 96 well plate as described above, had no effect on this 'single platelet' population (Figure 2b) consistent with data from traditional *ex vivo* aggregation assays where mixing alone does not cause platelet activation. Conversely, in the presence of classical platelet activating agonists such as collagen, the thrombin receptor (PAR4)-activating peptide, PAR4-amide, or the TxA_2-mimetic, U46619 there were marked depletions of the single platelet population (Figure 2c). Such losses of single platelets have been previously reported as measures of platelet aggregation[10-12]. By using enumeration beads to quantify the single platelet count per volume it was possible to accurately quantify depletion and make comparisons between samples. Using this approach, we recorded concentration-dependent losses of the single platelet population (Figure 2d – 2f). In response to 10µg/ml collagen stimulation 13±4% of single platelets remained, *i.e*. a maximal reduction of 87±4% with a co-efficient of variance (CV) of 16.1% (n=11). PAR4-amide stimulation led to a maximal loss of 79±5% (7.8% CV, n=9), and U46619 of 89±3% (7.4% CV, n=10). These agonists produced single platelet loss at concentrations that were similar to those previously

found to cause aggregation of mouse platelets in traditional assays[15,16]. To validate our observations we used a separate and distinct platelet marker, CD42d (GPV) and observed near identical platelet counts when we analysed separately for each marker over a range of activation conditions (r^2=0.998 by linear regression analysis; suppl. Figure 1).

We next went on to confirm if single platelet loss in stimulated whole blood is an active, inhibitable process. To do this, we pre-incubated blood with the powerful platelet inhibitor PGI_2, and found significant reductions in the single platelet depletion induced by maximal tested concentrations of all agonists: collagen, 87±4% of single platelet loss vs. 47±10 with PGI_2; PAR4-amide, 79±5% vs. 25±9%; and U46619, 89±2% vs. 26±7% (Figures 2d – 2f). These data demonstrate that the observed agonist-stimulated depletion of the single platelet population in this assay is an active process and not a result of chemical disruption or agglutination. It also demonstrates that the assay can detect the effect of inhibitory substances acting through platelet intracellular signalling pathways. Importantly, because each test condition requires only 35µl of blood, this panel of 3 agonists, each at 4 concentrations was testable using ~0.5ml of blood, half the total accessible blood volume of a mouse. Indeed, since a large sample volume remains after platelet counting for additional analyses, we also measured the formations of TxA_2 in response to collagen and separately to AA by immunoassay (suppl. Figure 2a, 2b), and found a clear association between the potencies of agonists as stimulants of TxA_2 formation and single platelet loss.

To explore the cause of agonist-induced loss of single platelets we examined unstimulated and collagen-stimulated mouse blood by confocal microscopy and imaging flow cytometry after immunofluorescent staining of platelets, leukocytes and erythrocytes. Vehicle-treated blood showed an abundance of single platelets and neutrophils with little interaction between cell types (Figure 2gi, 2gii). After stimulation with collagen, however, blood showed a depletion of single platelets together with the appearance of multiple large groups comprising platelet-platelet and platelet-leukocyte aggregates (Figures 2hi, 2hii) consistent with the associated single platelet depletion.

Having established a platelet-counting based activation assay in whole blood, we explored the applicability of the approach to studies in platelet-rich plasma. This preparation, although less physiological, can be valuable for platelet-focused studies in which other blood cells/components may confound the interpretation of results. Using the same assay conditions and measurement technique, mouse platelet-rich plasma behaved similarly to whole blood, showing concentration-dependent single platelet depletion in response to collagen, U46619 and PAR4-amide (suppl. Figure S3). The potency of these agonist and

sensitivity of detection as determined by platelet counting was similar to that recorded when aggregation was measured by the more conventional light transmission approach[8] (suppl. Figure S3). Finally, to confirm the suitability of this mouse whole blood assay to blood collected into different, more conventional anti-coagulants, we measured AA-, collagen-, PAR4-amide- and U46619-induced single platelet depletion responses in blood collected into sodium citrate or heparin. In both cases, we observed similar agonist-induced single platelet depletion responses as those described above for lepirudin anti-coagulated blood (suppl. Figure S4).

Detection of the anti-platelet effect of $P2Y_{12}$ receptor blockade and COX1-deficiency

After defining this assay, we wanted to consider its sensitivity to loss of known platelet signalling pathways. We examined the COX-1/TxA_2 and ADP-$P2Y_{12}$ receptor pathways since in contrast to PGI_2 their interruption produces a more modest and selective alteration in platelet responsiveness, and both directly translate to existing therapeutics in clinical use.

Prasugrel, like clopidogrel, is a blocker of the ADP-receptor $P2Y_{12}$[18-20]. It is well established that $P2Y_{12}$ blockade has significant effects upon platelet responsiveness to collagen, U46619 and PAR4 agonists consistent with its anti-thrombotic effect in man[21-23]. We found that the $P2Y_{12}$ receptor blocker prasugrel active metabolite (PAM, 3µM) markedly prevented agonist-induced single platelet loss, as compared to vehicle (0.5% DMSO). This inhibition persisted even at the highest concentrations tested of collagen (72±10% vs. 58±11%), PAR4-amide (80±4% vs. 11±6%), and U46619 (50±15% vs. 1±1%) (Figure 3a – 3c).

COX-1, the therapeutic target of aspirin, converts AA into prostaglandin H_2, a catalytic step required for the generation of TxA_2 by activated platelets. Using our assay we observed that platelets in blood from COX-1-deficient mice demonstrated a complete absence of the response to 0.1mM AA, whilst wild-type (WT) mice demonstrated a strong response (WT, 71±7% vs. KO, 1±2%). Platelet responses to collagen were also blunted in blood from COX-1-deficient mice, even at maximal concentrations (WT, 71±5% vs. KO, 34±13%; Figure 4a). In contrast, COX-1-deficiency had little effect on responses to PAR4-amide or U46619 (Figures 4b & 4c). Again, this is consistent with the established role of COX-1-derived TxA_2 in the response to collagen but not to thrombin receptor stimulation by PAR4-amide or exogenous thromboxane (U46619)[24-27].

The ability of the assay described here to detect reproducibly the anti-thrombotic effects of $P2Y_{12}$ receptor blockade and COX-1 gene deletion demonstrates its suitability for detecting specific defects in platelet signalling. Data from COX-1-deficient mice are particularly

relevant since screening and initial phenotyping of platelet function in genetically modified mice could be an important application of this assay. This data also highlights the importance of testing a range of platelet responses in parallel since COX-1 deletion selectively modifies responses to AA and collagen without affecting those to PAR4-amide and U46619. This is possible in the assay presented here because the blood volumes required for each test are very low, allowing study of multiple pathways in parallel to generate a broad response profile for each mouse tested.

Altered platelet phenotypes in mice lacking intercellular adhesion molecule (ICAM)-1

Having developed a robust mouse platelet function assay we next wanted to apply the technique to a novel biological question. Since a particular benefit of this assay is the ability to monitor platelet-leukocyte interactions in activated whole blood, we sought to screen mice deficient in specific leukocyte adhesion molecules to determine whether these adhesion molecules contribute to platelet-leukocyte and platelet-platelet interactions. Through this approach we found that deletion of ICAM-1 attenuates single platelet loss (wild-type: 39±14% vs. ICAM-1 KO: 14±8%; Figure 5a) in response to sub-maximal concentration of U46619. However when platelet function was studied in PRP no such differences were observed (suppl. Figure S5), demonstrating that the effect of ICAM-1 is dependent on blood cells/constituents other than platelets. ICAM-1, expressed on lymphocytes, neutrophils, monocytes and endothelial cells but not on platelets is known to play a key role in leukocyte transmigration through the endothelial cell layer[28,29]. Given we have established that platelet-leukocyte interactions play a role in the observed single platelet depletion and that we only observed an effect of ICAM-1 deletion on the response to the TXA_2 mimetic U46619, which unlike collagen and PAR4-amide, activates leukocytes as well as platelets, we reasoned ICAM-1 may be a mediator of platelet-monocyte binding. To confirm this we examined U46619-stimulated samples by flow cytometric imaging (Figure 5b). Upon quantification significantly less platelet-monocyte interactions were present in ICAM-1 KO mice compared to WT (WT: 41±1%; ICAM-1 KO: 27±2%; Figure 5c) suggesting that ICAM-1 may particularly drive platelet-monocyte interactions.

Basal monocyte ICAM-1 expression is relatively low but is greatly increased during inflammation[30]. We therefore sought to stimulate monocyte ICAM-1 induction by incubating whole blood with murine TNF-α, which led to a time-dependent increase in monocyte ICAM-1 immunoreactivity (suppl. Figure S6). mTNF-α treatment also increased 'basal' platelet-monocyte interactions, in both WT and ICAM-1 KO mouse blood. In blood primed with mTNF-α, U46619-induced platelet-monocyte adhesion in WT mouse blood was significantly increased from 41±1% to 58±3%. However, in blood from ICAM-1 KO mice, the ability of

mTNF-α to potentiate U46619-induced platelet-monocyte interactions was abolished (27±2% no mTNF-α vs 32±6% with mTNF-α; Figure 5c & 5d), indicating that the potentiation of U46619-induced platelet-monocyte association produced by mTNF-α is ICAM-1-dependent.

Lastly, we wanted to examine the mechanism of interaction between monocyte ICAM-1 and platelets. ICAM-1 mediates leukocyte-leukocyte interactions primarily by binding to lymphocyte function-associated antigen (LFA)-1. Although LFA-1 has been described on the mouse platelet surface it is present only at a low level[31]. ICAM-1 can also directly bind fibrinogen to mediate indirect leukocyte adhesion[32]. Given that activated platelets avidly bind fibrinogen by the glycoprotein (GP)IIb/IIIa complex we hypothesised this may also serve as a mechanism for ICAM-1-mediated platelet-leukocyte interactions. To test this we repeated previous experiments using U46619 and murine TNF-α with the addition of eptifibatide, a competitive inhibitor of fibrinogen binding to the platelet[2]. Under these conditions we found that the observed increases in platelet-monocyte interactions were reversed in WT blood (23±2%) to the levels observed in blood from ICAM-1 KO mice (27±2%; Figure 5c & 5d). Since eptifibitide inhibits only platelet fibrinogen binding, we also performed experiments in the presence of an excess of the fibrinogen γ-117–133 peptide sequence. This mimics the ICAM-1-binding sequence within fibrinogen[33,34] and thus actively compete with native fibrinogen[35] for monocyte ICAM-1 binding. We observed that in the presence of this excess peptide, platelet-monocyte interactions induced by U44619 and TNF-α were significantly decreased from 59±3% to 40±5% in WT mice, while there was no change in interactions observed in ICAM-1 KO mice (32±6% to 28±3%, Figure 5c). This supports the conclusion that fibrinogen acts as a ligand for ICAM-1-dependent platelet-monocyte binding.

These data identify a novel role of ICAM-1 in mediating platelet-monocyte interaction, particularly under conditions of inflammation (i.e. as modelled by addition of TNF-α). This raises questions as to whether ICAM-1 may also mediate platelet binding to other cell types such as neutrophils and endothelial cells and whether this mechanism may contribute to the role of platelets in vascular inflammation[36]. For example, platelet-leukocyte aggregates have been identified as key contributors to the pathogenesis of atherosclerosis[37], sepsis[38] and more recently, venous thrombosis[39].

Summary and conclusions

Here we have described and validated a low volume, 96-well plate based whole blood mouse platelet aggregation assay that has significant advantages over currently established assays. Firstly, by requiring only 35µl of blood per replicate it permits a higher number of

simultaneous tests to be conducted without the need for excessive platelet handling that can introduce artefacts. Secondly, this assay can readily be used for particular platelet-focused studies. Consequently, a detailed platelet phenotype informed by use of activators and inhibitors that signal through multiple intracellular signalling pathways can be revealed with the minimal use of animals. This not only provides a thorough understanding of platelet thrombotic pathways but may also be of value in identifying potential signalling defects that may reflect physiology in other cell types that are less accessible for testing. Here, our application of this assay to phenotype responses from ICAM-1 deficient mice and subsequent identification of ICAM-1, through binding fibrinogen, as being a novel mediator of platelet-monocyte interaction is demonstration of its utility. Moreover, this approach may be of particular use in prospective phenotyping of novel genetically modified mice such as those generated by knock-out mouse consortia [40,41]. In conclusion, the refined, robust and readily accessible assay we present here addresses an important scientific need by improving current experimental methodology for murine platelet testing.

Acknowledgements

This work was generously supported by the British Heart Foundation (PG/12/68/29779 and PG/14/48/30916) and the Wellcome Trust (101604/Z/13/Z to SN and TW, and 098291/Z/12/Z to S.N).

Authorship Contributions

PCJA designed the research, performed the assays and collected data, analysed and interpreted data, performed statistical analysis, and wrote the manuscript. NSK and MVC collected data, analysed and interpreted data and revised the manuscript. MF collected data. NH and SN contributed vital reagents and revised the manuscript. TDW designed the research, analysed and interpreted data and revised the manuscript.

Disclosure of Conflicts of Interest

There are no conflicts of interest to disclose.

Bibliography

1. Hirsh J, Buchanan MR, Ofosu FA, Weitz J. Evolution of thrombosis. *Ann N Y Acad Sci*. 1987;516:586-604.

2. Armstrong PC, Peter K. GPIIb/IIIa inhibitors: from bench to bedside and back to bench again. *Thromb Haemost*. 2012;107(5):808-814.

3. Patrono C, Andreotti F, Arnesen H, et al. Antiplatelet agents for the treatment and prevention of atherothrombosis. *Eur Heart J*. 2011;32(23):2922-2932.

4. Rand ML, Leung R, Packham MA. Platelet function assays. *Transfus Apher Sci*. 2003;28(3):307-317.
5. Harrison P, Frelinger AL, 3rd, Furman MI, Michelson AD. Measuring antiplatelet drug effects in the laboratory. *Thromb Res*. 2007;120(3):323-336.
6. Michelson AD. Methods for the measurement of platelet function. *Am J Cardiol*. 2009;103(3 Suppl):20A-26A.
7. Chan MV, Warner TD. Standardised optical multichannel (optimul) platelet aggregometry using high-speed shaking and fixed time point readings. *Platelets*. 2012;23(5):404-408.
8. Chan MV, Armstrong PC, Papalia F, Kirkby NS, Warner TD. Optical multichannel (optimul) platelet aggregometry in 96-well plates as an additional method of platelet reactivity testing. *Platelets*. 2011;22(7):485-494.
9. Lordkipanidze M, Lowe GC, Kirkby NS, et al. Characterization of multiple platelet activation pathways in patients with bleeding as a high-throughput screening option: use of 96-well Optimul assay. *Blood*. 2014;123(8):e11-22.
10. Konstantopoulos K, Wu KK, Udden MM, Banez EI, Shattil SJ, Hellums JD. Flow cytometric studies of platelet responses to shear stress in whole blood. *Biorheology*. 1995;32(1):73-93.
11. Turner NA, Moake JL, McIntire LV. Blockade of adenosine diphosphate receptors P2Y(12) and P2Y(1) is required to inhibit platelet aggregation in whole blood under flow. *Blood*. 2001;98(12):3340-3345.
12. Fox SC, Sasae R, Janson S, May JA, Heptinstall S. Quantitation of platelet aggregation and microaggregate formation in whole blood by flow cytometry. *Platelets*. 2004;15(2):85-93.
13. Alugupalli KR, Michelson AD, Barnard MR, Leong JM. Serial determinations of platelet counts in mice by flow cytometry. *Thromb Haemost*. 2001;86(2):668-671.
14. Kirkby NS, Lundberg MH, Harrington LS, et al. Cyclooxygenase-1, not cyclooxygenase-2, is responsible for physiological production of prostacyclin in the cardiovascular system. *Proc Natl Acad Sci U S A*. 2012;109(43):17597-17602.
15. Xu H, Gonzalo JA, St Pierre Y, et al. Leukocytosis and resistance to septic shock in intercellular adhesion molecule 1-deficient mice. *J Exp Med*. 1994;180(1):95-109.
16. Woulfe D, Jiang H, Morgans A, Monks R, Birnbaum M, Brass LF. Defects in secretion, aggregation, and thrombus formation in platelets from mice lacking Akt2. *J Clin Invest*. 2004;113(3):441-450.
17. Cattaneo M, Hayward CP, Moffat KA, Pugliano MT, Liu Y, Michelson AD. Results of a worldwide survey on the assessment of platelet function by light transmission aggregometry: a report from the platelet physiology subcommittee of the SSC of the ISTH. *J Thromb Haemost*. 2009;7(6):1029.
18. Warner TD, Nylander S, Whatling C. Anti-platelet therapy: cyclo-oxygenase inhibition and the use of aspirin with particular regard to dual anti-platelet therapy. *Br J Clin Pharmacol*. 2011;72(4):619-633.
19. Cattaneo M. The platelet P2Y(1)(2) receptor for adenosine diphosphate: congenital and drug-induced defects. *Blood*. 2011;117(7):2102-2112.
20. Iyu D, Glenn JR, White AE, Fox SC, Heptinstall S. Adenosine derived from ADP can contribute to inhibition of platelet aggregation in the presence of a P2Y12 antagonist. *Arterioscler Thromb Vasc Biol*. 2011;31(2):416-422.
21. Armstrong PC, Leadbeater PD, Chan MV, et al. In the presence of strong P2Y12 receptor blockade, aspirin provides little additional inhibition of platelet aggregation. *J Thromb Haemost*. 2011;9(3):552-561.
22. Shankar H, Garcia A, Prabhakar J, Kim S, Kunapuli SP. P2Y12 receptor-mediated potentiation of thrombin-induced thromboxane A2 generation in platelets occurs through regulation of Erk1/2 activation. *J Thromb Haemost*. 2006;4(3):638-647.

23. Paul BZ, Jin J, Kunapuli SP. Molecular mechanism of thromboxane A(2)-induced platelet aggregation. Essential role for p2t(ac) and alpha(2a) receptors. *J Biol Chem*. 1999;274(41):29108-29114.
24. Armstrong PC, Truss NJ, Ali FY, et al. Aspirin and the in vitro linear relationship between thromboxane A2-mediated platelet aggregation and platelet production of thromboxane A2. *J Thromb Haemost*. 2008;6(11):1933-1943.
25. Armstrong PC, Kirkby NS, Zain ZN, Emerson M, Mitchell JA, Warner TD. Thrombosis is reduced by inhibition of COX-1, but unaffected by inhibition of COX-2, in an acute model of platelet activation in the mouse. *PLoS One*. 2011;6(5):e20062.
26. Nakamura T, Kambayashi J, Okuma M, Tandon NN. Activation of the GP IIb-IIIa complex induced by platelet adhesion to collagen is mediated by both alpha2beta1 integrin and GP VI. *J Biol Chem*. 1999;274(17):11897-11903.
27. di Minno G, Bertele V, Bianchi L, et al. Effects of any epoxymethano stable analogue of prostaglandin endoperoxides (U-46619) on human platelets. *Thromb Haemost*. 1981;45(2):103-106.
28. Kevil CG, Patel RP, Bullard DC. Essential role of ICAM-1 in mediating monocyte adhesion to aortic endothelial cells. *Am J Physiol Cell Physiol*. 2001;281(5):C1442-1447.
29. Ley K, Laudanna C, Cybulsky MI, Nourshargh S. Getting to the site of inflammation: the leukocyte adhesion cascade updated. *Nat Rev Immunol*. 2007;7(9):678-689.
30. Freyer D, Manz R, Ziegenhorn A, et al. Cerebral endothelial cells release TNF-alpha after stimulation with cell walls of Streptococcus pneumoniae and regulate inducible nitric oxide synthase and ICAM-1 expression via autocrine loops. *J Immunol*. 1999;163(8):4308-4314.
31. McCaffery PJ, Berridge MV. Expression of the leukocyte functional molecule (LFA-1) on mouse platelets. *Blood*. 1986;67(6):1757-1764.
32. Languino LR, Plescia J, Duperray A, et al. Fibrinogen mediates leukocyte adhesion to vascular endothelium through an ICAM-1-dependent pathway. *Cell*. 1993;73(7):1423-1434.
33. Altieri DC, Duperray A, Plescia J, Thornton GB, Languino LR. Structural recognition of a novel fibrinogen gamma chain sequence (117-133) by intercellular adhesion molecule-1 mediates leukocyte-endothelium interaction. *J Biol Chem*. 1995;270(2):696-699.
34. D'Souza SE, Byers-Ward VJ, Gardiner EE, Wang H, Sung SS. Identification of an active sequence within the first immunoglobulin domain of intercellular cell adhesion molecule-1 (ICAM-1) that interacts with fibrinogen. *J Biol Chem*. 1996;271(39):24270-24277.
35. Languino LR, Duperray A, Joganic KJ, Fornaro M, Thornton GB, Altieri DC. Regulation of leukocyte-endothelium interaction and leukocyte transendothelial migration by intercellular adhesion molecule 1-fibrinogen recognition. *Proc Natl Acad Sci U S A*. 1995;92(5):1505-1509.
36. Projahn D, Koenen RR. Platelets: key players in vascular inflammation. *J Leukoc Biol*. 2012;92(6):1167-1175.
37. Huo Y, Schober A, Forlow SB, et al. Circulating activated platelets exacerbate atherosclerosis in mice deficient in apolipoprotein E. *Nat Med*. 2003;9(1):61-67.
38. Clark SR, Ma AC, Tavener SA, et al. Platelet TLR4 activates neutrophil extracellular traps to ensnare bacteria in septic blood. *Nat Med*. 2007;13(4):463-469.
39. von Bruhl ML, Stark K, Steinhart A, et al. Monocytes, neutrophils, and platelets cooperate to initiate and propagate venous thrombosis in mice in vivo. *J Exp Med*. 2012;209(4):819-835.
40. Threadgill DW, Churchill GA. Ten Years of the Collaborative Cross. *G3: Genes|Genomes|Genetics*. 2012;2(2):153-156.
41. Abbott A. Mouse project to find each gene's role. *Nature*. 2010;465(7297):410.

Figure Legends

Figure 1: Schematic diagram of methodology. Whole blood is removed from the vena cava of an anaesthetised mouse, aliquoted into an agonist containing 96-well plate, before mixing at 37°C for 5 mins. Subsequently, blood is sampled from each well, diluted and stained using specific anti-platelet antibodies. Quantitative beads are then added before single platelet counts are acquired.

Figure 2: Concentration-dependent loss of single platelets following agonist stimulation due to formation of platelet-platelet and platelet-leukocyte aggregates. Representative dot plots of platelet populations and quantitative gating, as identified by anti-CD41 APC antibody staining in, A) unmixed blood and B) vehicle mixed samples remains stable. Platelet population was depleted in C) agonist (collagen 1µg/ml) mixed samples. Platelet loss occurred in a concentration-dependent manner following treatment with increasing concentrations of the common agonists D) collagen, E) PAR4-amide AYPGKF, and F) U46619. Loss was significantly reduced by inclusion of prostacyclin (Epoprostenol, 2µg/ml). Analysis of Gi) vehicle-stimulated and Hi) collagen-stimulated whole blood acquired using an ImagestreamX MarkII incorporating a x 60 objective lens, scale bars equal to 7µm identified platelet-platelet and platelet-leukocyte aggregates. Platelets identified by anti-CD41 (green), leukocytes by anti-CD45 (yellow) and erythrocytes by anti-Ter119 (red). Confocal imaging of Gii) vehicle-treated and Hii) collagen-stimulated samples, with subsequent erythrocyte-lysis, confirmed respective absence and presence of stimulated platelet (CD42c, green)-platelet and platelet-neutrophil (MRP-14, red) aggregates. Images were acquired in 3D by confocal microscopy using a Zeiss LSM 5 PASCAL confocal laser-scanning microscope incorporating a x 63 oil-dipping objective lens (numerical aperture 1.4) and the image acquisition software IMARIS. Scale bars equal to 20µm. Data reported as mean ± SEM (n=3-11), *p<0.05 by paired t-test.

Figure 3: Sensitivity of assay to $P2Y_{12}$ inhibition. Pre-treatment of whole blood with the $P2Y_{12}$ receptor blocker prasugrel active metabolite (PAM, 3µM) inhibited the platelet response to A) 1µg/ml collagen, B) PAR4-AP, or C) U46619. Data reported as mean ± SEM (n=6). *p<0.05 by two way ANOVA versus vehicle (0.5% DMSO).

Figure 4: Phenotype of COX-1 knock-out mice. Responses of platelets in blood from COX-1 knockout mice, compared to wild type mice, were significantly inhibited for A) collagen, and for lower concentrations of B) PAR4 amide or C) U46619. Data reported as mean ± SEM (n=6). *p<0.05 by two way ANOVA.

Figure 5: Phenotypic analysis of ICAM-1 knock-out mice and role in platelet-monocyte interaction. Platelet reactivity in blood from ICAM-1 knockout mice, compared to wild type mice, were no different following A) collagen or PAR4 amide stimulation but significantly inhibited in response to 0.3µM U46619 (n=6 for all). B) Flow cytometric imaging (x60

objective) of samples stimulated by U46619 (0.3μM) revealed a potential difference in platelet (green) monocyte (red) interactions. Scale bars equal to 7μm. C) Quantitation of these interactions identified significantly more platelet-monocyte interactions upon U46619 stimulation in wild-type compared to ICAM-1 KO mice. In wild-type mice this interaction was exaggerated when blood was pre-stimulated with mTNF-α but reversed when performed in the additional presence of eptifibatide, or the fibrinogen peptide γ-117–133. The level of interaction in ICAM-1 KO mice remained constant through all conditions (n=3 for all). D) Corresponding representative histograms of platelet (CD42d-PE) binding of the Ly6C (monocyte) positive population in WT (left) and KO (right) mice in absence (red) and presence (blue) of eptifibatide. Data presented as mean ± SEM, *$p<0.05$ by two-way ANOVA.

Figure 1

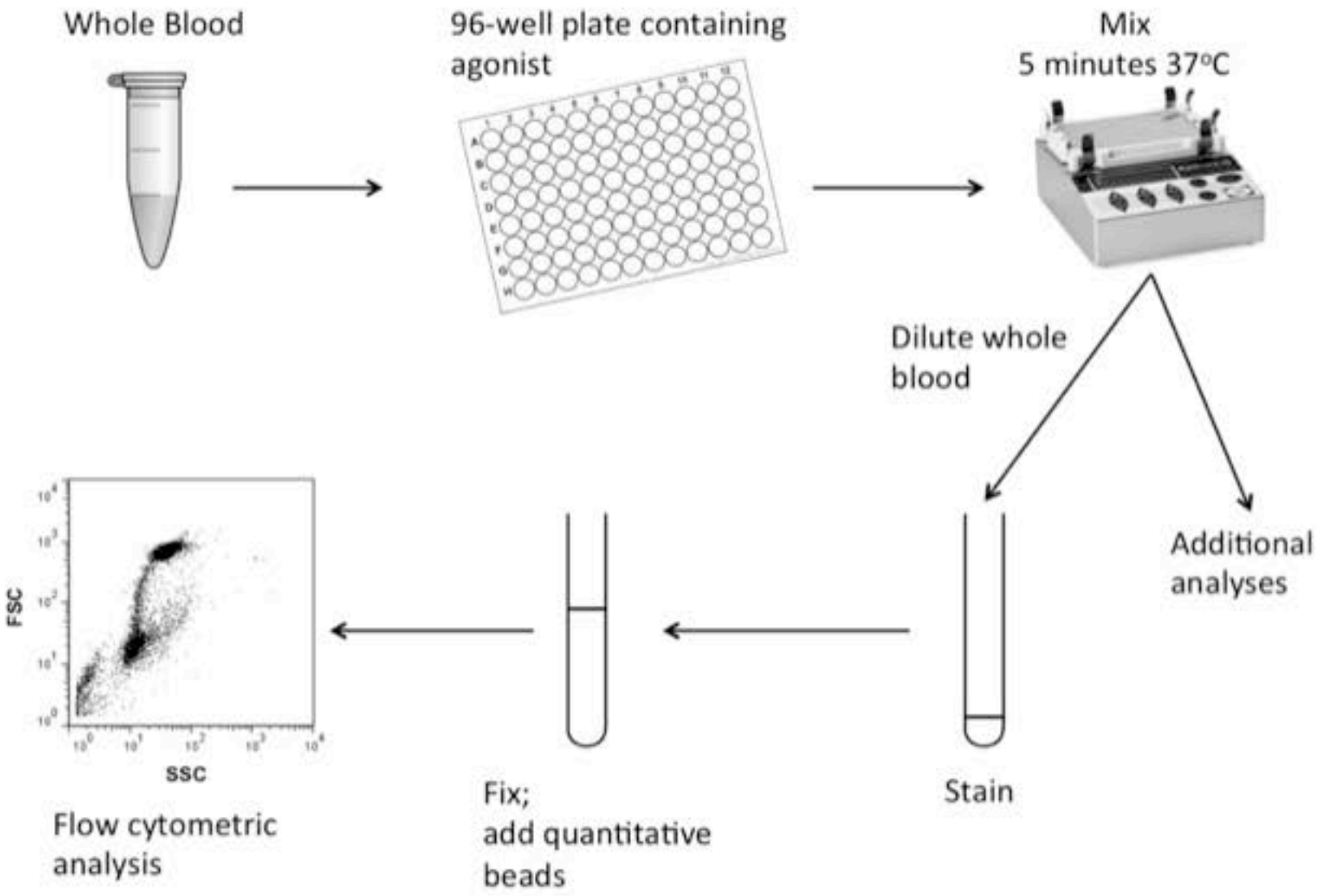
Whole Blood
96-well plate containing agonist
Mix
5 minutes 37°C
Dilute whole blood
Additional analyses
FSC
ssc
Flow cytometric analysis
Fix;
add quantitative beads
Stain

Figure 2

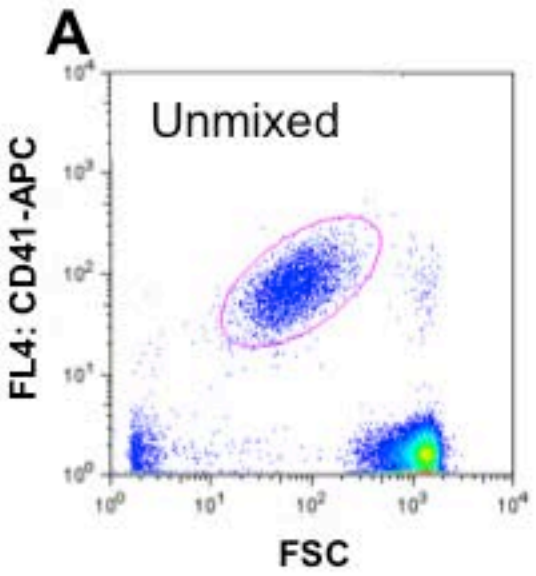
A
Unmixed
FL4: CD41-APC
FSC

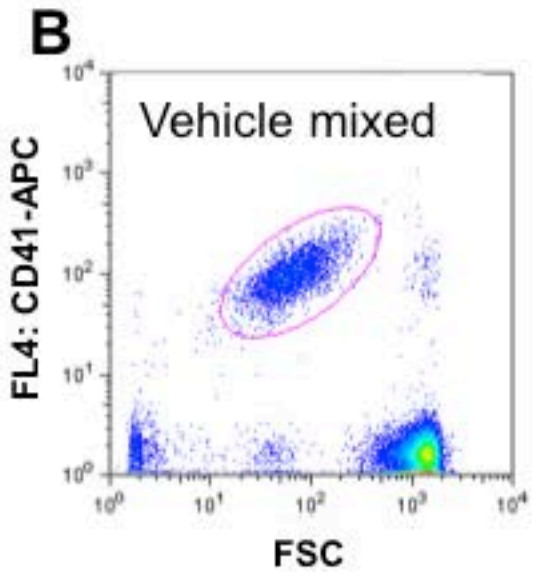
B
Vehicle mixed
FL4: CD41-APC
FSC

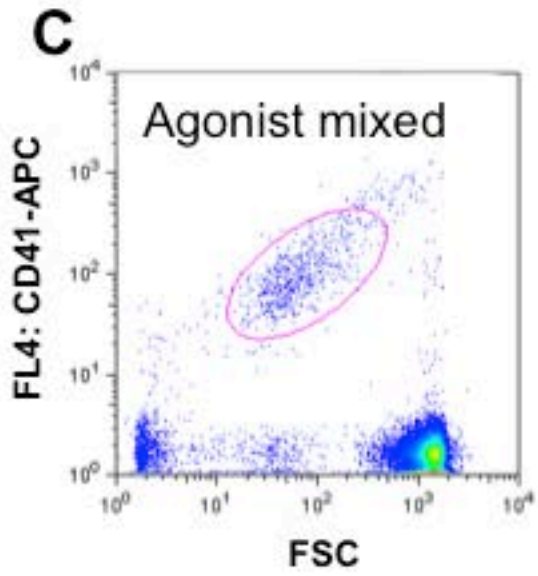
C
Agonist mixed
FL4: CD41-APC
FSC

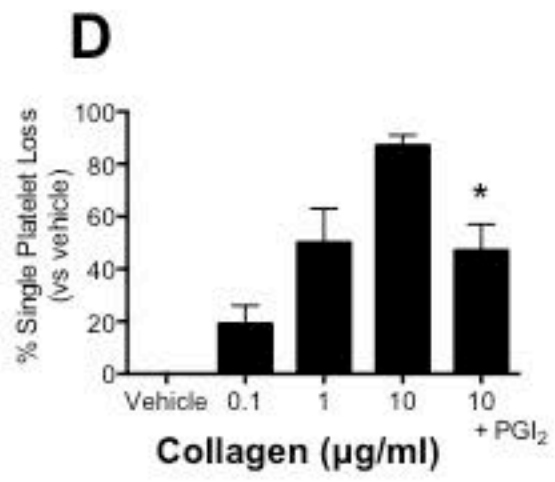
D
% Single Platelet Loss (vs vehicle)
Vehicle
0.1
1
10
10 + PGI2
Collagen (µg/ml)

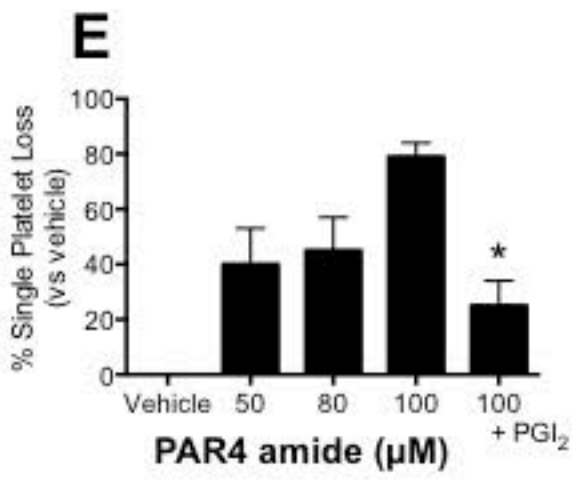
E
% Single Platelet Loss (vs vehicle)
Vehicle
50
80
100
100 + PGI2
PAR4 amide (µM)

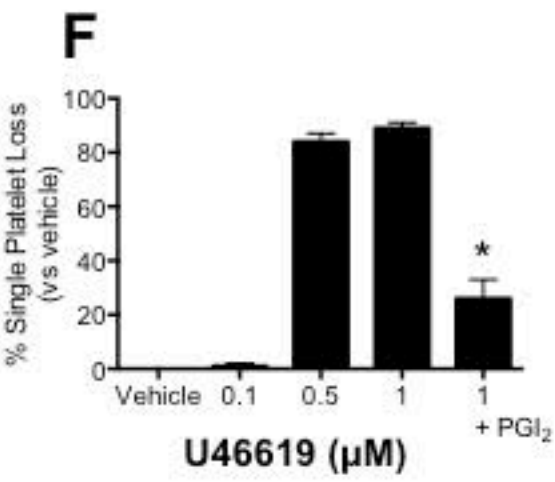
F
% Single Platelet Loss (vs vehicle)
Vehicle
0.1
0.5
1
1 + PGI2
U46619 (µM)

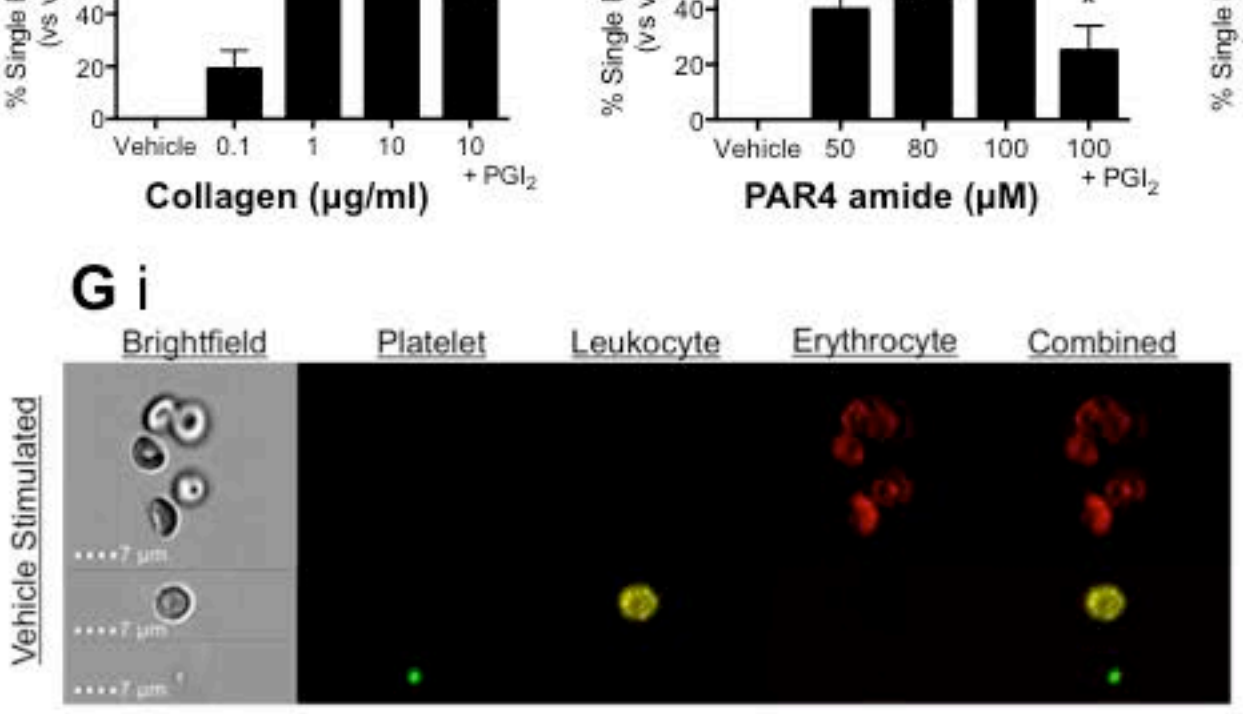
G i
Brightfield
Platelet
Leukocyte
Erythrocyte
Combined
Vehicle Stimulated
7 µm

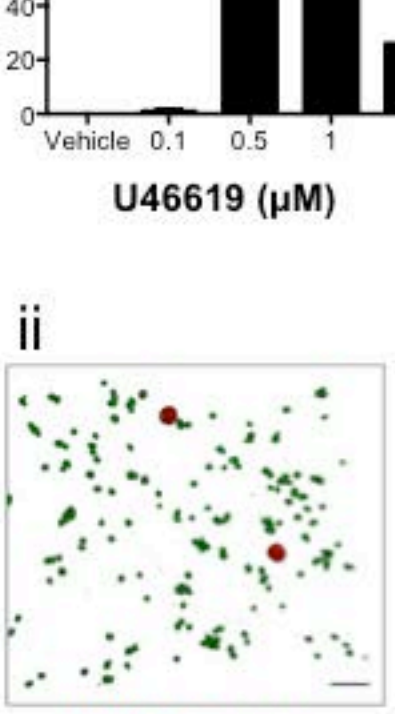
ii
MRP-14, CD42c

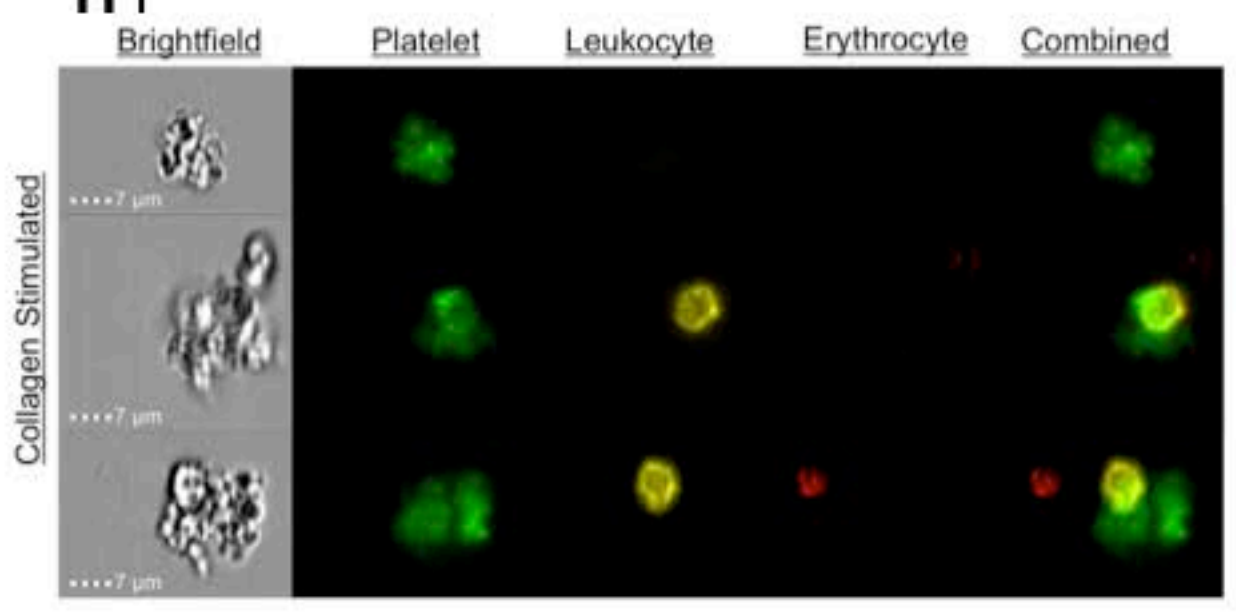
H i
Brightfield
Platelet
Leukocyte
Erythrocyte
Combined
Collagen Stimulated
7 µm

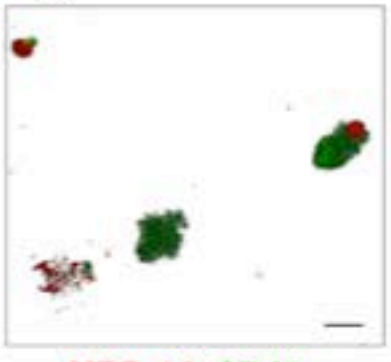
ii
MRP-14, CD42c

Figure 3

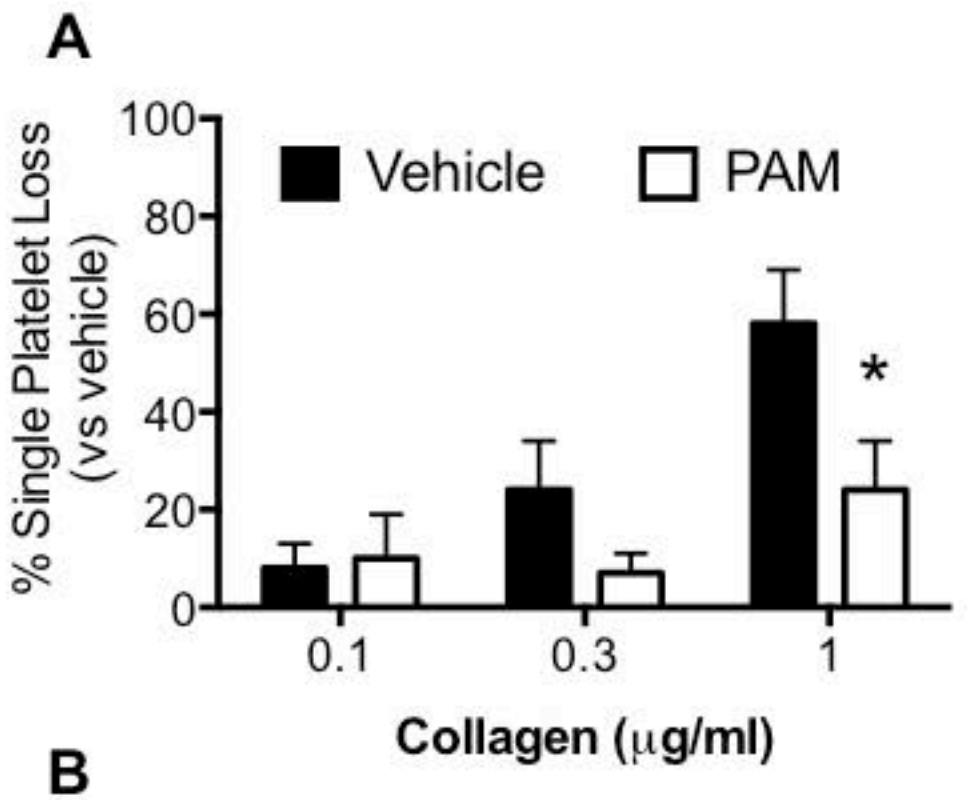
A
% Single Platelet Loss (vs vehicle)
100
80
60
40
20
0
Vehicle
PAM
*
0.1
0.3
1
Collagen (μg/ml)

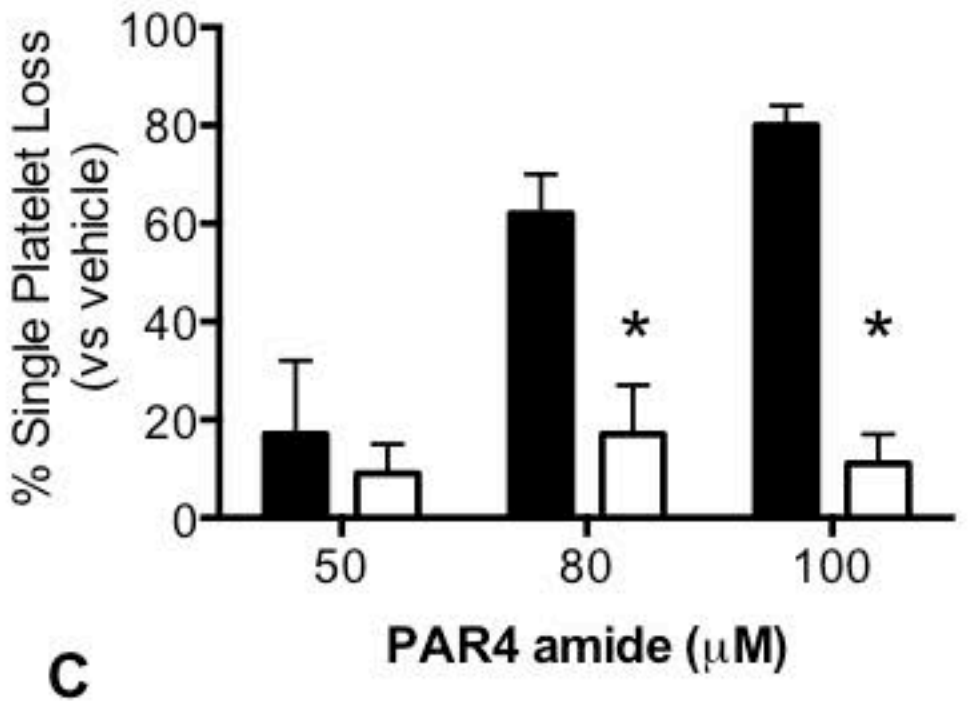
B
% Single Platelet Loss (vs vehicle)
100
80
60
40
20
0
*
*
50
80
100
PAR4 amide (μM)

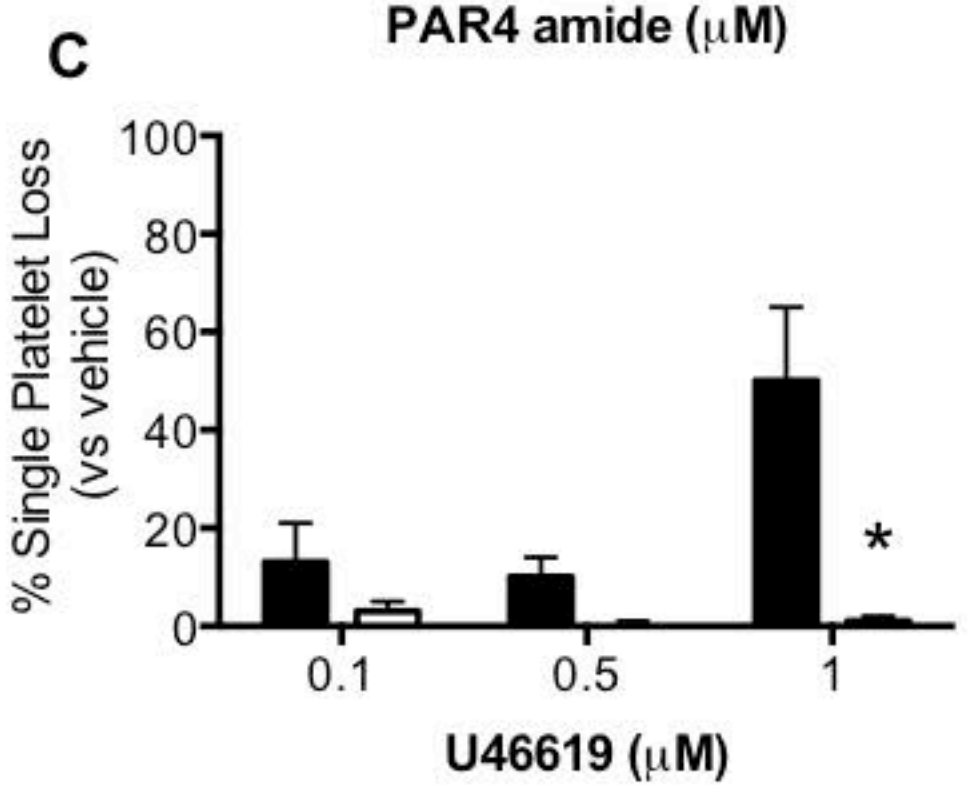
C
% Single Platelet Loss (vs vehicle)
100
80
60
40
20
0
*
0.1
0.5
1
U46619 (μM)

Figure 4

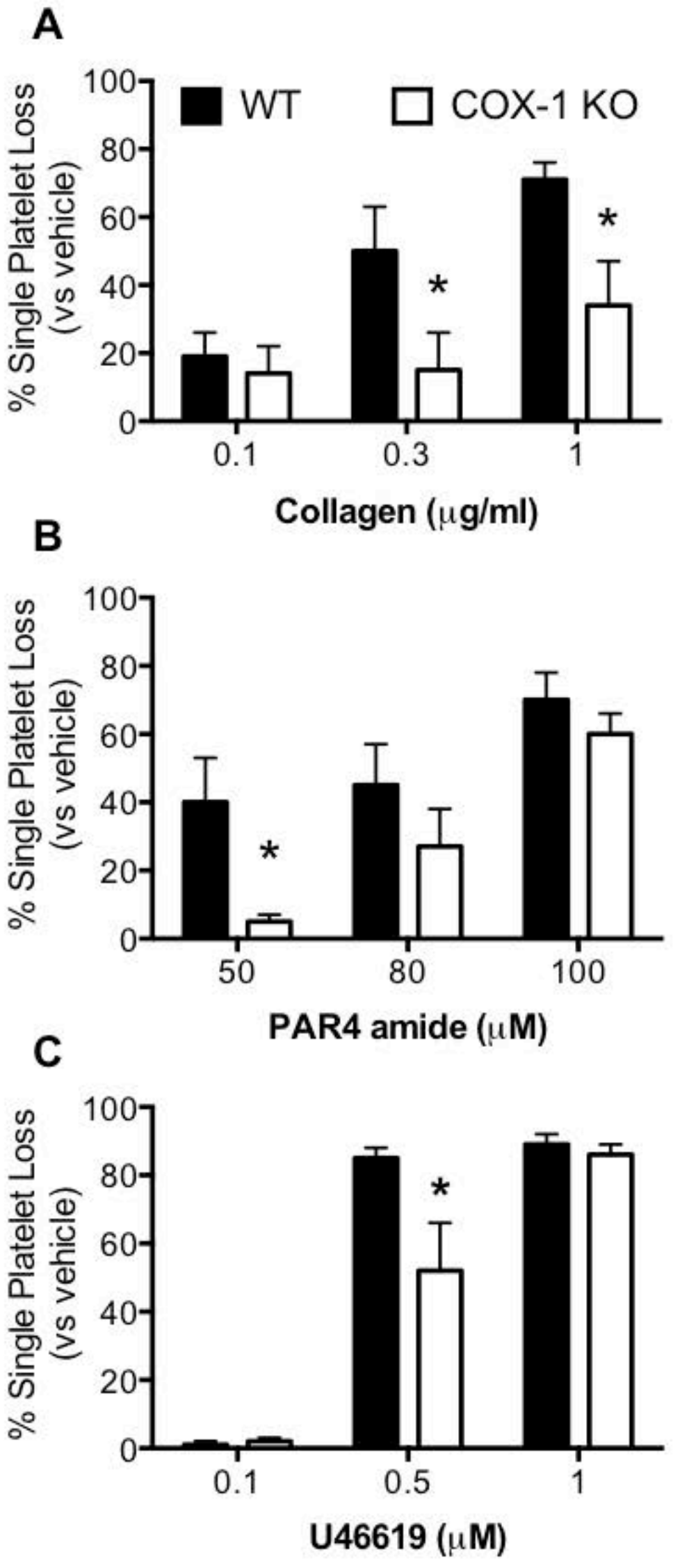
A
WT
COX-1 KO
% Single Platelet Loss (vs vehicle)
100
80
60
40
20
0
*
*
0.1
0.3
1
Collagen (μg/ml)
B
% Single Platelet Loss (vs vehicle)
100
80
60
40
20
0
*
50
80
100
PAR4 amide (μM)
C
% Single Platelet Loss (vs vehicle)
100
80
60
40
20
0
*
0.1
0.5
1
U46619 (μM)

Figure 5

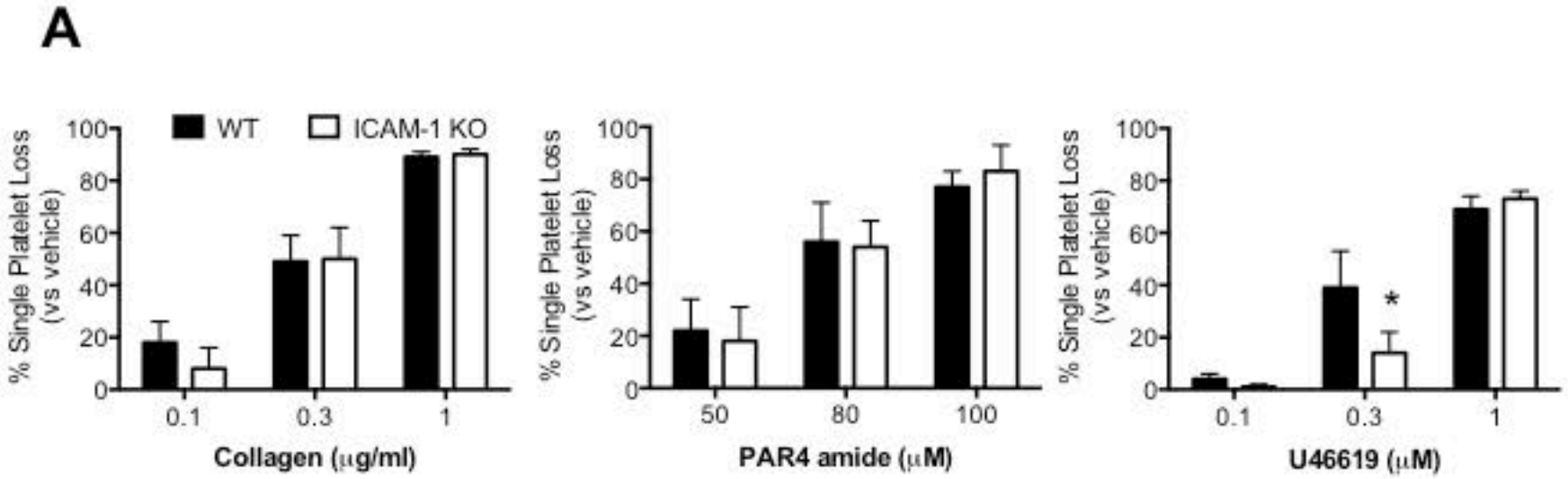
A
WT
ICAM-1 KO
% Single Platelet Loss (vs vehicle)
Collagen (μg/ml)
PAR4 amide (μM)
U46619 (μM)
*

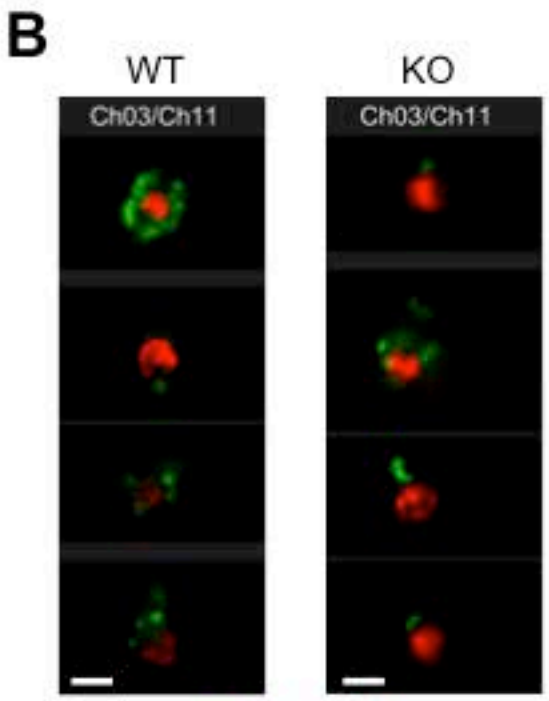
B
WT
KO
Ch03/Ch11
CD41, Ly6C

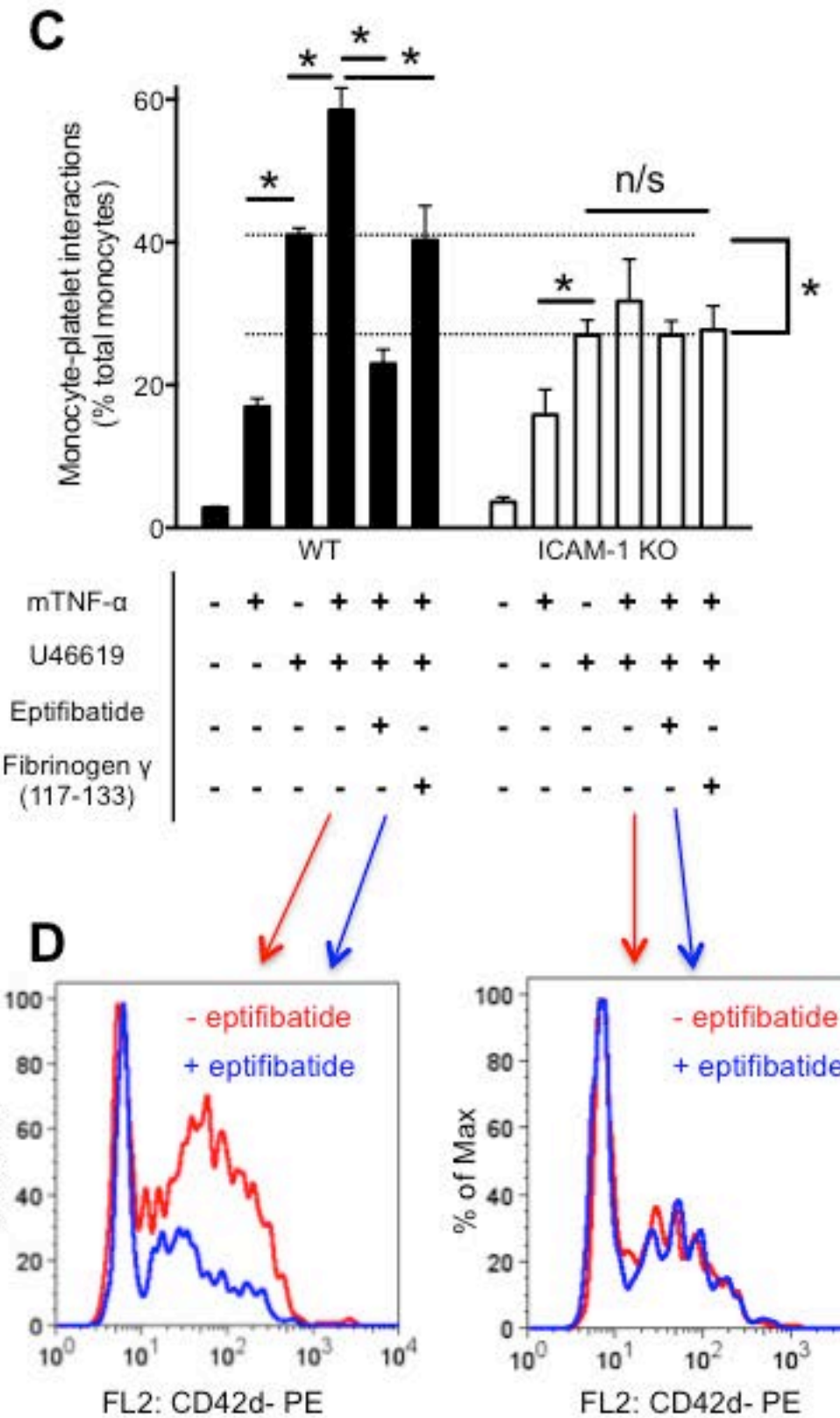
C
Monocyte-platelet interactions (% total monocytes)
n/s
WT
ICAM-1 KO
mTNF-α
U46619
Eptifibatide
Fibrinogen γ (117-133)
D
- eptifibatide
+ eptifibatide
% of Max
FL2: CD42d- PE